Specific heat from 0.4 to 7 K and magnetization from 2 to 40 K of samarium

Specific heat from 0.4 to 7 K and magnetization from 2 to 40 K of samarium

S J Collocott† and A M Stewart‡

† CSIRO Division of Applied Physics, Lindfield, NSW 2070, Australia
‡ Department of Applied Mathematics, The Australian National University, Canberra, ACT 2601, Australia

Abstract. Measurements of the specific heat from 0.4 to 7 K have been made on two polycrystalline specimens of samarium of different purity. There are differences in the specific heat of the two specimens between 2 and 7 K which are attributed to differing magnetic contributions. Below 2 K, both specimens show a small specific heat anomaly that is most likely due to samarium oxide. For samarium, a value for the electronic specific heat of 9 ± 2 mJ mol^{-1} K^{-2} is obtained. Magnetization measurements on the two specimens between 2 and 40 K show a large peak at 13.7 K. A smaller peak in the magnetization, corresponding to that in the specific heat, is observed at 20.4 K in the purer specimen.

1. Introduction

The rare-earth metal samarium crystallizes with rhombohedral symmetry, and the structure can be envisaged as a nine-layer stacking sequence ABABCBCAC of hexagonal close packed layers, with two thirds of the atoms having local hexagonal symmetry and the remainder local cubic symmetry [1]. At 106 K the hexagonal sites undergo a transition from a paramagnetic to a collinear antiferromagnetic state, whilst the cubic sites order below about 14 K [1]. The moments of both sites lie along the c-axis [1]. These magnetic transitions have been investigated by specific heat [2–6] and magnetic [7–9] studies. Interest has not only been confined to the temperature regions where the magnetic transitions occur, but also to the specific heat of Sm below 4 K [10–12], where impurities in rare-earth metals, particularly oxide impurities, are known to affect markedly the determination of the electronic specific heat [13].

Our earlier specific heat study [6] on the same two specimens of samarium, which are of different purity, covered the range 2–32 K, and focused on the specific heat anomaly at 13.7 K associated with magnetic ordering of the cubic sites. The measurements showed marked differences between the two specimens. The peak at 13.7 K in the specimen of higher purity was sharper, and about 1.6 times greater in magnitude than in the less pure specimen. There was an additional small peak at 20.4 K present in the higher-purity specimen, which was visible only as a diffuse bump in the less pure specimen (to our knowledge, this was the first time this peak had been reported). Both specimens had a small specific heat anomaly at 9.6 K of unknown origin.

In this study we extend the specific heat measurements to lower temperatures, and present new data from 0.4 to 7 K. The objective of these measurements was to see if differences observed at the 13.7 K magnetic transition, and at the 20.4 K peak, manifest themselves in a temperature region where impurities are known to have a marked effect on the specific heat of rare-earth metals. The specific heat measurements are complemented with magnetization measurements from 6 to 40 K to probe any magnetic anomalies associated with the specific heat anomalies at 9.6, 13.7 and 20.4 K. The examination of the same polycrystalline Sm specimens by specific heat and magnetization measurements should assist in clarifying whether some of the observed anomalies are intrinsic or impurity related.

2. Experiment

The two polycrystalline Sm specimens were the same specimens as used in our earlier study [6], denoted Sm IV and Sm V. Specimen Sm IV was prepared by the Ames Laboratory (Iowa State University, Ames, IA, USA) and was of 99.89 at.% purity (including gaseous impurities); it was dehydrogenated to 0.01 at.% hydrogen at Ames and then heat treated at 550 °C in ultra-high vacuum. Specimen Sm V was supplied as Sublimed Grade from Rare Earth Products (Widness, Cheshire, UK) and stated to be of 99.98% purity, excluding gaseous impurities. Sm V was purchased prior to 1980 and is likely to have a higher level of gaseous impurities than more recently produced specimens. Sm V was consolidated by RF melting on a copper hearth under purified argon [5]. Both Sm specimens were analysed by inductively coupled plasma mass spectrometry (ICPMS), and no significant differences were detected with the exception that Sm V contained 160 PPM by weight Mn compared to 1 PPM by weight in Sm IV. As ICPMS does not give any information on the oxides of Sm, both specimens were examined using a scanning electron microscope equipped with an energy dispersive x-ray analysis facility. The sensitivity limit for this technique is of order 0.5 at.%, and oxides at this level were just detected in both specimens. It should be pointed out that an oxide impurity of less than 100 PPM can produce significant errors in the low-temperature specific heat [13].

The specific heat measurements from 0.4 to 7 K were made by a semi-adiabatic heat pulse method [14], in the ^{4}He–^{3}He cryostat used for the earlier measurements from 2 to 32 K. The only change was that the germanium resistance thermometer (GRT), which is part of the addenda, used for the 2 to 32 K measurements was replaced by a more appropriate GRT for the 0.4 to 7 K temperature range. The specific heat of the addenda was measured in a separate experiment, so that corrections for the addenda could be made to the Sm measurements. The accuracy of the calorimeter was checked by specific heat measurements of the 1965 Calorimetry Conference reference material (see Osborne *et al* and Holste *et al* [15]), and our values agree with the measurements of Holste *et al* [15] within an overall inaccuracy of ±0.4%. Both Sm specimens were cleaned by etching for a few seconds in dilute caustic soda followed by surface abrasion with steel wool to remove any visible trace of surface oxides before the specific heat measurements were made. The DC magnetization measurements were made using a commercial SQUID-based magnetometer system. Each specimen was cooled in zero magnetic field from a a temperature well above 106 K to 6 K, the magnetic field was then applied and the measurements were made as the temperature increased.

3. Results

3.1. Specific Heat

Results for the specific heat, C_p, for both Sm IV and Sm V are shown in figure 1 as a plot of C_p against T on a double-logarithmic scale. Included for comparison in figure 1 are the C_p data in the region of temperature overlap of our earlier 2 to 32 K study [6], the C_p data of Lounasmaa [10] (runs IA and IB) and the C_p data of Anderson *et al* [11]. There is broad agreement between all sets of C_p data above 2 K, though the C_p data for Sm IV lie below those for Sm V (see figure 2 for greater detail). Below 2 K differences become most apparent on the background of the nuclear hyperfine specific heat, C_{hfs}, which becomes an increasingly larger fraction of the total C_p. At 0.4 K C_{hfs} dominates and all the C_p data sets converge. In the region 0.4 to 2 K it is evident that there is an extra contribution to C_p for both Sm IV and Sm V, which is larger for Sm IV. Also, the C_p data for Sm IV from this work do not join smoothly with the data from our earlier study in the region 1.5 to 2 K. This is perplexing as it does not occur with the Sm V data, and identical measurement techniques were used for the two specimens. Although both specimens were covered in grease and stored under a dry nitrogen atmosphere to minimize oxidation, and cleaned before making measurements, Sm IV may have deteriorated in storage in the years between the experiments, with the formation of a small amount of samarium oxide the likely cause.
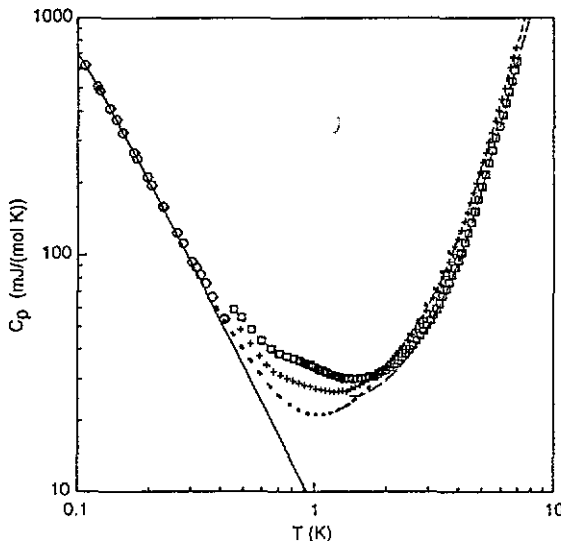

Figure 1. C_p against T for samarium: □, Sm IV; +, Sm V; ●, Lounasmaa [10] (runs IA and IB); ○, Anderson *et al* [11]. For clarity the data from our earlier 2 to 32 K study [6] are represented by curves: ----, Sm IV; – – –, Sm V. The solid line is the calculated nuclear hyperfine specific heat.

The C_p data below 7 K are interpreted by first subtracting the C_{hfs} contribution, and then determining the relative electronic, lattice, magnetic and impurity contributions to the non-hyperfine residue, $C_p - C_{hfs}$. C_{hfs} was computed for each experimental point assuming a normal isotopic abundance of 15% of ^{147}Sm and 13.84%

of ^{149}Sm using the following magnetic dipole and electric quadropole interaction parameters, a' and P (for each isotope), respectively,

$$a'_{147} = -0.0283 \pm 0.0008 \text{ K} \qquad P_{147} = -0.0002 \pm 0.0003 \text{ K}$$
$$a'_{149} = -0.0233 \pm 0.0007 \text{ K} \qquad P_{149} = +0.00005 \pm 0.00008 \text{ K}$$

given by Anderson et al [11] (see also Bleaney [16] and Hill et al [17] for the calculation method). The calculated C_{hfs} is included in figure 1 and $C_p - C_{hfs}$ against T for both Sm IV and Sm V are shown in figure 2. The electronic contribution is proportional to T, but as Sm is antiferromagnetically ordered below 14 K, both the magnetic and lattice contributions are assumed to be proportional to T^3, preventing separation of their relative contributions. Additionally, there will be departures from a simple T^3 behaviour as the magnetic transition temperature is approached, necessitating an upper temperature limit for any data fitting somewhat below the transition temperature. No simple temperature dependence can be ascribed to the impurity contribution, which appear in the $C_p - C_{hfs}$ data for both Sm IV and Sm V as diffuse 'bumps' centred about 1 K (see figure 2).
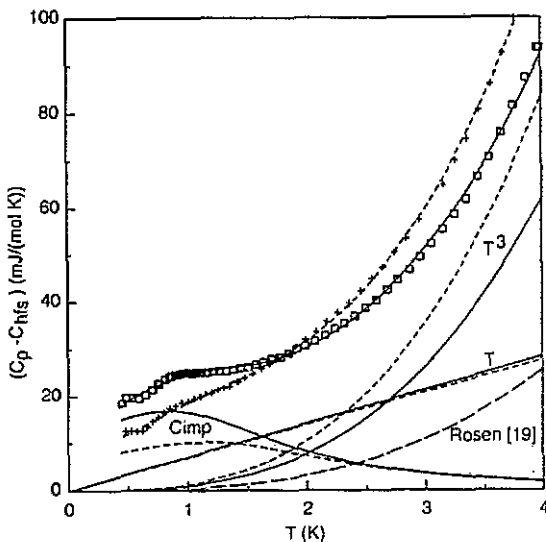

Figure 2. $C_p - C_{hfs}$ against T for Sm IV (□) and Sm V (+). Included are the fitted curves for Sm IV (solid curve) and Sm V (short-dash curve) to equation (1) using the parameters given in table 1 for a 'Lorentzian' impurity contribution. Also, shown are the individual contributions from the various terms (C_{imp} above 0.45 K, the T and T^3 (lattice + magnetic) contributions) for Sm IV (solid curves) and Sm V (short-dash curves). The lattice contribution to C_p for samarium from Rosen [18] for a Debye temperature of 169 K is shown by the long-dash curve.

The $C_p - C_{hfs}$ data from 0.4 to 4 K were fitted using the method of non-linear least-squares to

$$C_p - C_{hfs} = C_{imp}(T) + \gamma T + bT^3 \tag{1}$$

in mJ mol^{-1} K^{-1}, where γ is the coefficient of the electronic C_p, b the coefficient of the T^3 (lattice + magnetic) term and $C_{imp}(T)$ an arbitrary function to model the impurity contribution. The fitting procedure was performed using Schottky, Lorentzian

and Gaussian functions for $C_{imp}(T)$, and no special physical significance should be attached to any particular function. The advantage of this approach is that all data down to 0.4 K are used in the fitting procedure, but it has the limitation that an assumption is made for modelling the impurity contribution. To check if this assumption is reasonable the lower limit of the fit was truncated to 1.5 K, i.e., above the diffuse 'bump' at 1 K (see figure 2), and the data fitted to the expression, $aT^{-2} + \gamma T + bT^3$. Table 1 gives the values for the various parameters derived from the fits, the temperature range over which the data were fitted and the %RMS deviation of the fit. Fitted curves are included in figure 2. The values for γ and b for each specimen are reasonably consistent, regardless of choice of $C_{imp}(T)$ or if the fit is truncated to 2 K. This is not surprising as the impurity contribution to C_p is a small fraction of the total C_p. The values of γ for both Sm IV and Sm V are of similar magnitude, 9 ± 2 mJ mol^{-1} K^{-2} (cf 12.1 mJ mol^{-1} K^{-2} [10]), but there are differences in b which is consistently smaller in Sm IV, 0.88 to 1.01 mJ mol^{-1} K^{-4}, compared to Sm V, 1.02 to 1.33 mJ mol^{-1} K^{-4} (cf 0.877 to 1.113 mJ mol^{-1} K^{-4} [10]). The discrepancies in b reflect the different magnetic contributions in Sm IV and Sm V. Using the value of 169 K for the Debye temperature, determined by Rosen [18] from elastic constant measurements, we calculate the magnetic contribution to the total C_p at 4 K for Sm IV and Sm V to be $\approx 33\%$ and $\approx 50\%$, respectively.

Table 1. Fitting parameters for Sm IV and Sm V (units are mJ, mol and K).

	$C_{imp}(T)$	a	γ	b	%RMS	Temperature range
Sm IV	Gaussian	–	9.00	0.88242	2.39	0.4–4
	Lorentzian	–	7.13	0.97205	2.18	0.4–4
	Schottky	–	9.62	0.75887	4.63	0.4–4
	T^{-2}-term	32.86	6.76	1.0080	2.52	1.5–4
Sm V	Gaussian	–	7.25	1.3308	2.63	0.4–4
	Lorentzian	–	6.94	1.3108	2.63	0.4–4
	Schottky	–	10.57	1.0214	4.37	0.4–4
	T^{-2}-term	25.99	7.00	1.3263	2.71	1.5–4

A similar value for γ is obtained for Sm IV and Sm V, which suggests the two specimens are of similar purity, as studies on other rare-earth metals, e.g. Gd (Hill *et al* [19]), have shown that the measured γ decreases as specimen purity increases. This is despite the fact that Sm IV has a lower level of gaseous impurities. Both specimens show an impurity contribution near 1 K, which is more pronounced in Sm IV. Whilst the C_p data below 4 K indicate the presence of impurities, most probably samarium oxide, it is not clear whether these impurities are responsible for differences in the magnetic contribution to C_p above 2 K, or to C_p at the magnetic transition at 13.7 K.

3.2. Magnetization

The magnetizations, M, for both samples are shown in figures 3 and 4, plotted as M/H (dimensionless as M is in units of A m^{-1}, $\rho_{Sm} = 7.54$ g cm^{-3}) against T, for two values of the applied magnetic field H equal to 795.8 kA m^{-1} and 3 978.9 kA m^{-1}. Also shown in these figures are the specific heat data from our earlier study [6]. For the purer specimen Sm IV (figure 3) the two curves coincide,

indicating that its magnetization is linear with field. There is a main peak at 14 K and a small bump at 21 K. The main peak of M is a few tenths of a degree above the corresponding peak of the specific heat, in accordance with the prediction of Fisher [20]. The 20.4 K bump in M coincides with the minor peak in the specific heat. There is no discernible feature of M that corresponds to the small specific heat bump at 9.5 K.
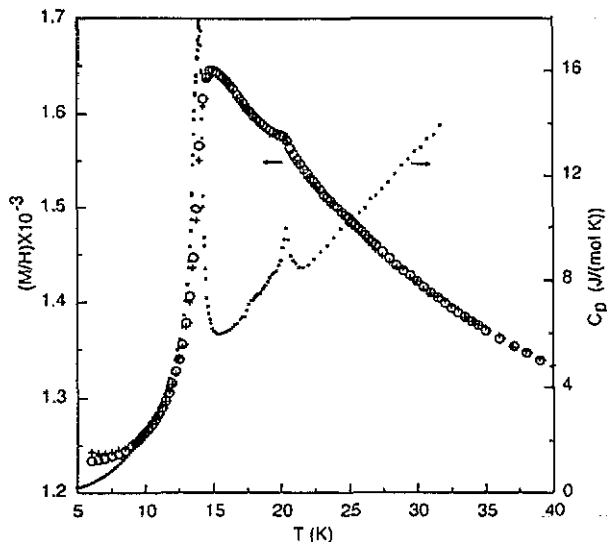

Figure 3. Magnetization, M, for the purer polycrystalline Sm IV plotted as M/H, dimensionless (left-hand vertical axis), against T for $H = 795.8$ kA m^{-1} (+) and $H = 3\,978.9$ kA m^{-1} (O). Also included is C_p (right-hand axis) against T (●) for Sm IV from our earlier study [6].

The two magnetization curves for the less pure specimen Sm V, in contrast, do not coincide, indicating non-linearity of the magnetization–field relation. The is no discernible bump at 20.4 K, corresponding to the one in the specific heat, and also none at 9.4 K.

4. Discussion and conclusion

Between 0.5 K and 1.5 K the specific heat of samarium is very sample-dependent. The most likely cause of this is oxide or hydride inclusions. Neither would have been detected by the methods we have used to analyse the composition of our specimens. Samarium oxide has two structural forms, cubic and monoclinic. The cubic form remains unordered down to 12 K [21]. The monoclinic form has been reported to remain unordered down to 2 K [22]. Measurements of greater resolution that we have made of its magnetization (figure 5) show no anomalies down to 6 K. Gadolinium oxide orders at 3.5 K (monoclinic) and 1.6 K (cubic) and the ordering temperature is sensitive to oxide stoichiometry [23]. If the ordering mechanism is exchange, and scales with the de Gennes factor, then the ordering temperature of the two samarium oxides should be 1 K and 0.5 K respectively; if the mechanism is dipole–dipole then the ordering temperatures will be much lower. The ordering temperature of samarium hydride is less than 4 K [24].
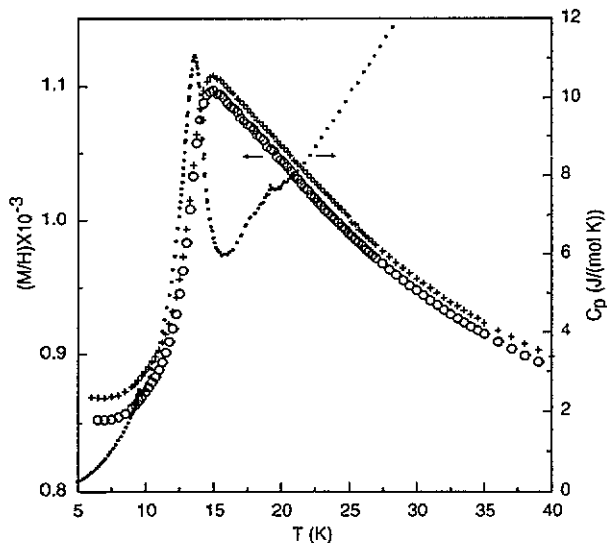
Figure 4. Magnetization, M, for the less pure Sm V plotted as M/H, dimensionless (left-hand vertical axis), against T for $H = 795.8$ kA m^{-1} (+) and $H = 3\,978.9$ kA m^{-1} (O). Also included is C_p (right-hand axis) against T (●) for Sm V from our earlier study [6].
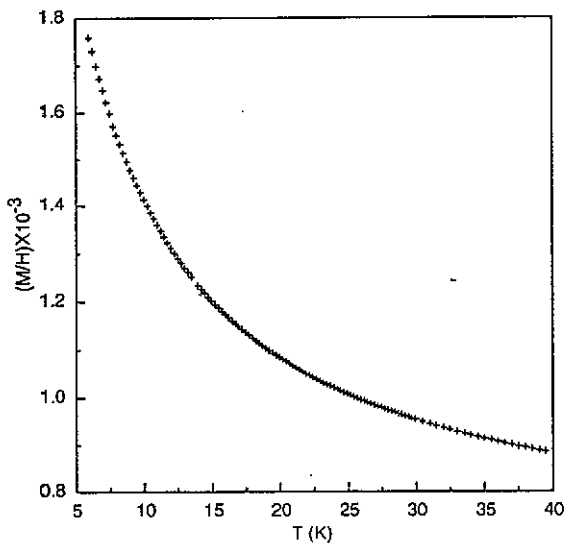

Figure 5. Magnetization, M, of monoclinic Sm$_2$O$_3$ ($\rho = 7.43$ g cm^{-3}) powder plotted as M/H, dimensionless, against T for applied field $H = 79.58$ kA m^{-1}.

The broad anomaly that we observe in the specific heat of both specimens at around 1 K is in the region where the oxides and hydrides might be expected to order magnetically. That we observe broad rather than sharp peaks may be attributed to varying structures and stoichiometries of the oxide or hydride defect complexes.

The hyperfine anomaly in the specific heat is well accounted for by theory. The coefficient of the electronic term in the specific heat is slightly less than that obtained previously [10, 12]. The main peak at 14 K in both the magnetization and specific

heat is associated with the ordering of the cubic sites [1]. The purer specimen Sm IV has the sharper peak. The peak at 21 K appears both in the specific heat and the magnetization, but the peak at 9.4 K appears only in the specific heat. These temperatures are too high to be associated with oxides or hydrides and so the anomalies, i.e. 9.4 and 21 K, are likely to be intrinsic and possibly due to a spin reorientation transition. The broad peak around 1 K is more likely to be extrinsic and caused by oxide or hydride defect complexes.

Acknowledgments

Note added in proof. Further magnetization measurements on SM IV have shown that the magnitude of M, the small bump at 21 K and the linear behaviour of the magnetization are sensitive to the orientation of the specimen in the field, and from where in the ingot the specimen was cut. The shape of the M/H against T curves are unchanged, but the peak M/H value may decrease to 1.2×10^{-3} (dimensionless). The susceptibility in Sm is known to be highly anisotropic [8], and these effects may indicate preferential alignment of crystals in the polycrystalline ingot.

References

[1]   Koehler W C and Moon R M 1972 *Phys. Rev. Lett.* **29** 1468
[2]   Roberts L M 1957 *Proc. Phys. Soc.* **70** 434
[3]   Jennings L D, Hill E D and Spedding F H 1959 *J. Chem. Phys.* **31** 1240
[4]   Lounasmaa O V and Sundström L J 1967 *Phys. Rev.* **158** 591
[5]   Jayasuriya K D, Stewart A M and Campbell S J 1986 *Mater. Chem. Phys.* **14** 525
[6]   Stewart A M and Collocott S J 1989 *J. Phys.: Condens. Matter* **1** 677
[7]   Lock J M 1957 *Proc. Phys. Soc.* B **70** 566
[8]   McEwen K A, Touborg P F, Cock G J and Roeland L W 1974 *J. Phys. F: Met. Phys.* **4** 2264
[9]   Arajs S, Rao K V, Hedman L and Åström 1975 *J. Low Temp. Phys.* **21** 197
[10] Lounasmaa O V 1962 *Phys. Rev.* **126** 1352
[11] Anderson A C, Holmström, Krusius M and Pickett G R 1969 *Phys. Rev.* **183** 546
[12] Lounasmaa O V and Veuro M C 1972 *Phys. Lett.* **40A** 371
[13] Hill R W 1986 *J. Phys. C: Solid State Phys.* **19** 673
[14] Collocott S J 1983 *Aust. J. Phys.* **36** 573
[15] Osborne D W, Flotow H E and Schreiner 1967 *Rev. Sci. Instrum.* **38** 159
      Holste J C, Cetas T C and Swenson C A 1972 *Rev. Sci. Instrum.* **43** 670
[16] Bleaney B 1963 *J. Appl. Phys.* **34** 1024
[17] Hill R W, Cosier J and Hukin D A 1976 *J. Phys. F: Met. Phys.* **6** 1731
[18] Rosen M 1969 *Phys. Rev.* **180** 540
[19] Hill R W, Collocott S J, Gschneidner K A Jr and Schmidt F A 1987 *J. Phys. F: Met. Phys.* **17** 1867
[20] Fisher M E 1962 *Phil. Mag.* **7** 1731
[21] Perakis N and Kern K 1972 *C.R. Acad. Sci., Paris* B **1275** 677
[22] Borovik-Romanov A S and Kreines N M 1956 *Sov. Phys.-JETP* **2** 657
[23] Miller A E, Jelinek F J, Gschneidner K A Jr and Gertstein B C 1971 *J. Chem. Phys.* **55** 2647
[24] Kubota Y and Wallace W E 1963 *J. Appl. Phys.* **34** 1348